

# UC Irvine

## UC Irvine Previously Published Works

### Title

Control Design for a Bottoming Solid Oxide Fuel Cell Gas Turbine Hybrid System

### Permalink

<https://escholarship.org/uc/item/23h9f9bm>

### Journal

Journal of Electrochemical Energy Conversion and Storage, 4(3)

### ISSN

1550-624X

### ISBN

9780791837801

### Authors

Mueller, Fabian  
Jabbari, Faryar  
Brouwer, Jacob  
[et al.](#)

### Publication Date

2007-08-01

### DOI

10.1115/1.2713785

### Copyright Information

This work is made available under the terms of a Creative Commons Attribution License, available at <https://creativecommons.org/licenses/by/4.0/>

Peer reviewed

## FUELCELL2006-97150

### CONTROL DESIGN FOR A BOTTOMING SOLID OXIDE FUEL CELL GAS TURBINE HYBRID SYSTEM

Fabian Mueller, Faryar Jabbari, Jacob Brouwer, and Rory Roberts  
National Fuel Cell Research Center, University of California at Irvine, Irvine, CA  
Email: fm@nfcrc.uci.edu; fjabbari@uci.edu; jb@nfcrc.uci.edu; rar@nfcrc.uci.edu

Tobias Junker<sup>†</sup> and Hossein Ghezel-Ayagh  
FuelCell Energy, Inc., 3 Great Pasture Road, Danbury, CT  
Email: tjunker@fce.com; hghezel@fce.com  
<sup>†</sup>Corresponding author: Phone: 203-825-6056, Fax: 203-825-6273

#### ABSTRACT

A bottoming 275 kilowatt planar solid oxide fuel cell (SOFC) gas turbine (GT) hybrid system control approach has been conceptualized and designed. Based on previously published modeling techniques, a dynamic model is developed that captures the physics sufficient for dynamic simulation of all processes that affect the system with time scales greater than ten milliseconds. The dynamic model was used to make system design improvements to enable the system to operate dynamically over a wide range of power output (15 to 100% power). The wide range of operation was possible by burning supplementary fuel in the combustor and operating the turbine at variable speed for improved thermal management.

The dynamic model was employed to design a control strategy for the system. Analyses of the relative gain array (RGA) of the system at several operating points gave insight into input/output (I/O) pairing for decentralized control. Particularly, the analyses indicate that for SOFC/GT hybrid plants that use voltage as a controlled variable it is beneficial to control system power by manipulating fuel cell current and to control fuel cell voltage by manipulating the anode fuel flowrate. To control the stack temperature during transient load changes, a cascade control structure is employed in which a fast inner loop that maintains the GT shaft speed receives its setpoint from a slower outer loop that maintains the stack temperature. Fuel can be added to the combustor to maintain the turbine inlet temperature for the lower operating power conditions. To maintain fuel utilization and to prevent fuel starvation in the fuel cell, fuel is supplied to the fuel cell proportionally to the stack current. In addition, voltage is used as an indicator of varying fuel concentrations allowing the fuel flow to be adjusted accordingly. Using voltage as a sensor is shown

to be a potential solution to making SOFC systems robust to varying fuel compositions.

The simulation tool proved effective for fuel cell/GT hybrid system control system development. The resulting SOFC/GT system control approach is shown to have transient load-following capability over a wide range of power, ambient temperature, and fuel concentration variations.

Keywords: SOFC hybrid, gas turbine, control design, system design, robust control, RGA

#### INTRODUCTION

Because of high efficiency and low pollutant emissions characteristics, solid oxide fuel cell/gas turbine (SOFC/GT) hybrid systems are receiving increasingly more attention as potential future electric power generators. The Department of Energy has been supporting the development of SOFC/GT hybrids for distributed generation as well as large scale stationary power applications [1, 2]. Regardless of the application, hybrid systems in practice will need to be robust to ambient temperature and fuel concentration variations. In addition, hybrid systems that are efficient over a wide power operating range and that have load following capability will be much more attractive.

Consequently, transient control research of hybrid systems has been receiving some attention in the literature [3–5]. Prior control designs have been designed for molten carbonate fuel cell/GT hybrid systems, and topping SOFC/GT hybrid systems but none have been studied for bottoming SOFC/GT hybrid systems. Due to the complexity and nonlinearity of hybrid systems, hybrid control research has not tended to utilize traditional linear control theory [5, 6]. Instead, the approach has been decentralized multi-loop feedforward–feedback type

controllers, designed and evaluated by means of trial and error and/or dynamic modeling. It has been determined that even though there are strong interactions between the manipulated and controlled variables in the system, a decentralized multi-loop control design can be made stable because of the differing times scales of each control loop [5].

The present control strategy, designed for a bottoming SOFC/GT hybrid system, is consistent with prior controls research. It is a decentralized multi-loop feedforward–feedback type controller. The final system design contains four main controllers to maintain safe operation of the system: A system power controller, a cascaded GT shaft speed/fuel cell temperature controller, a combustor temperature controller, and an anode fuel flow controller. Many of the control concepts applied in the present research have been investigated previously, but not in the configuration presented here or for the case of controlling a bottoming SOFC/GT hybrid system. Particularly, the present research makes use of system linearization, and relative gain array analysis to select a system control configuration and input-output pairing of the system. In addition, careful attention has been paid to the design of the fuel flow controller. The final system control design is found: (1) to be robust to ambient temperature and fuel concentration variations, (2) to have rapid load following capability, and (3) to have a wide range of system operating power.

## NOMENCLATURE

$A$	Surface Area [ $\text{m}^2$ ]
$C$	Specific heat capacity [ $\text{kJ kg}^{-1} \text{K}^{-1}$ ]
$C_v$	Constant volume specific heat capacity [ $\text{kJ kmol}^{-1} \text{K}^{-1}$ ]
$E_{ohm}$	Ohmic polarization [V]
$F$	Faraday's constant [ $96,487 \text{ C mol}^{-1}$ ]
$h$	Enthalpy [ $\text{kJ kmol}^{-1}$ ]
$i$	Electrical current [A]
$J$	Polar moment of inertia [ $\text{kg m}^2$ ]
$N$	Molar capacity, or total number of moles [kmol]
$\dot{N}$	Molar flow rate [ $\text{kmol sec}^{-1}$ ]
$n$	Total number of cells in the stack(s) [-]
$P$	Power [kW], Pressure [KPa]
$\dot{Q}$	Heat transfer [kW]
$R$	Universal gas constant [ $8.3145 \text{ kJ kmol}^{-1} \text{K}^{-1}$ ] Control volume reaction rate [ $\text{kmol sec}^{-1}$ ]
$T$	Temperature [K]
$t$	Time [sec]
$U$	Fuel utilization [-]
$V$	Volume [ $\text{m}^3$ ], Voltage [V]
$\dot{W}$	Work out of control volume [kW]
$X$	Species mole fraction [-]
Greek Letters	
$\Theta$	Theoretical hydrogen mole fraction [-]
$\rho$	Density of solid [ $\text{kg m}^{-3}$ ]
$\omega$	Angular velocity [ $\text{rad sec}^{-1}$ ]

## Subscripts

$fc$	Fuel cell
$i$	Species [ $\text{CH}_4 \text{ CO CO}_2 \text{ H}_2 \text{ H}_2\text{O N}_2 \text{ O}_2$ ]
$in$	Control volume inlet
$mgt$	Micro gas turbine
$set$	Set point
$out$	Control volume outlet

## SYSTEM CONFIGURATION

To design an effective control strategy it is important to understand the system design, system component interactions and system operating requirements. The analyzed 275 kW bottoming SOFC/GT hybrid system is shown in Figure 1. The principal function of the system is to provide electrical power. The fuel cell is the core system component, because it generates most of the system power (87% of the total system power at maximum power) and because it has significant control requirements and constraints. The fuel cell in the system is a planar anode supported SOFC. To provide hydrogen rich synthesis gas to individual SOFC cells, the fuel cell stack contains planar reformer channels in series with cells in the stack. As shown in Figure 1, the water needed for reformation is provided externally. This simplifies control of the steam to carbon ratio as compared to recycling water from the anode exhaust [7, 8]. This requires a fuel heater to preheat fuel and water before entering the fuel cell.

Other system components support operation of the fuel cell. The gas turbine generates supplementary power (very important in terms of efficiency), but from a control perspective the gas turbine's primary purpose is to provide air flow to the fuel cell. Air flow to the fuel cell is of crucial importance, not only because it provides oxygen for the electrochemical reaction but also because it cools the stack in addition to the cooling effect of the endothermic internal reformation. To control the fuel cell temperature, the amount of air flow through the cathode is controlled. In the current system, this is accomplished by operating the turbine at variable speeds. Such design has been investigated systematically and shown beneficial for hybrid systems by many [3–5, 9–10].

This leads to the above mentioned cascade control structure: The GT shaft speed is controlled in a fast inner loop. It receives its setpoint from the slow outer loop that controls the stack temperature. Because the inner loop is fast in comparison, it can reject disturbances such as ambient temperature changes, before they affect the temperature control loop.

Downstream of the fuel cell, unreacted fuel is oxidized in a combustor. The system configuration allows for supplementary fuel flow to the combustor to maintain a high combustor temperature, and consequently a high turbine inlet temperature. Note that a heat exchanger is used following the combustor to transfer heat from the combustor exhaust to the turbine inlet air.

Use of supplementary combustor fuel has been studied in detail by [12] for a topping SOFC/GT hybrid, showing that such a strategy enhances the operating conditions of the gas turbine and improves turbine performance. For a bottoming cycle, supplementary fuel to the combustor is further advantageous, because it maintains the cathode inlet temperature. If the combustor temperature increases, then so does the heat exchanger temperature, the turbine inlet temperature, and, after expansion, the cathode inlet temperature. Therefore, if the combustor inlet temperature is increased, so is the cathode inlet temperature. The supplementary combustor fuel serves as a cathode pre-heater. This is particularly important to maintain the fuel cell temperature in part load conditions when the fuel cell tends to cool down due to reduced heat generation within the cells.

It is essential that the system operate safely at all times. To ensure safe operation of the system, the following system operating requirements and limitations are used in the control design:

- (1) The maximum fuel cell temperature must always be less than 1073 K, so metal interconnects can be used [13].
- (2) The temperature difference between the cathode inlet temperature and the fuel cell electrolyte temperature must be less than 200 K. To avoid thermal stresses in the fuel cell, this temperature difference must be minimized. Note that a 200 K temperature difference might be too large for a practical system depending upon the design, material set, and length of the fuel cell [14].
- (3) Hydrogen must not be depleted in the anode. The hydrogen mole fraction must always be greater than 0.01. The fuel cell potential is highly dependent on the concentration of the electrochemically active species. In addition, if the fuel (hydrogen) becomes depleted, an irreversible anode oxidation can occur.
- (4) Due to material restrictions the combustor temperature must not exceed 1150 K.
- (5) The maximum gas turbine shaft speed is 97,000 RPM.

The control strategy presented herein is designed to ensure the system is operating within the above specified requirements at all times regardless of ambient temperature, fuel concentration variations, or system load transients.

## MODEL

A dynamic model of the hybrid system, as presented in Figure 1 and described in the previous section was constructed in MATLAB/Simulink<sup>®</sup>. To facilitate linearization using MATLAB's built-in linearization commands, the nonlinear state space model was constructed free of any algebraic loops<sup>1</sup>. Note that the linear model was only used in the present research for the

<sup>1</sup> In MATLAB, an algebraic loop occurs, when a function's input depends on its own output. To compute the output, MATLAB requires iterations which significantly slows down the simulation. Also, systems with algebraic loops cannot be linearized using MATLAB's *linmod* command.

relative gain array (RGA) analyses used to determine optimal control structure and input output pairing. The system model was constructed using a physical modeling approach similar to that developed in [16–18], applied to the present system. Because the focus of this paper is control design, the dynamic model is only described briefly. Model details relevant to the system linearization are explained in detail. The overall system model comprises 64 nonlinear coupled ordinary differential equations as well as associated nonlinear constitutive equations. Accordingly, the linearized model has 64 states.

## HEAT EXCHANGER

The heat exchangers in the system are modeled as flat plate counter flow heat exchangers as presented in [16, 18]. Each heat exchanger is discretized into hot and cold streams and the plate separating the two streams. The three control volumes are then used to discretize the heat exchanger into five nodes in the stream-wise direction. Note that this discretization is particularly important for the combustor/turbine heat exchanger due to significant thermal gradients between the inlet and outlet streams of that heat exchanger.

The temperature and species mole fractions in gas control volumes of the heat exchanger, as well as the combustor, reformer, and fuel cell model are determined from solution of the dynamic energy and species conservation equations in the general form:

$$NC_v \frac{dT}{dt} = \dot{N}_{in} h_{in} - \dot{N}_{out} h_{out} + \sum \dot{Q}_{in} - \sum \dot{W}_{out} \quad (1)$$

$$N \frac{dX_i}{dt} = \dot{N}_{in} X_{i,in} - \dot{N}_{out} X_{i,out} + R_i \quad (2)$$

and the temperature of solid control volumes is found from solving the dynamic solid-state energy conservation equation in the general form:

$$\rho VC \frac{dT}{dt} = \sum \dot{Q}_{in} - \sum \dot{W}_{out} \quad (3)$$

Convection heat transfer between each stream and the plate is modeled using Newton's law of cooling, and Fourier's law is used to model conduction heat transfer along the heat exchanger plate.

## COMBUSTOR

The combustor is modeled as a single control volume as presented in [17, 18]. The combustor contains three inlet streams (i.e., anode exhaust, combustor fuel, and cathode exhaust) and a single exhaust stream. To simplify the model, the combustor is assumed to operate adiabatically with complete fuel oxidation. Then the exit mole fractions can be determined from Equation (2) and the outlet temperature from Equation (1). The thermal capacitance associated with the mass of combustor and catalyst is included in the energy conservation equation.

## FUEL CELL

Each cell unit in the stack, i.e., cathode gas, cathode, electrolyte, anode, anode gas, separator plates (interconnects), and indirect internal reformer, is assumed to operate identically, such that simulation of a single cell unit is taken as representative of the entire stack performance. To avoid algebraic loops in the electrochemical model as explained in [17, 18], the fuel cell was not discretized in the flow direction. Instead, the cathode gas, electrode-electrolyte assembly, anode gas, separator plate, and indirect internal reformer stream each represent a single bulk control volume of the fuel cell model. Convection heat transfer is modeled between each gas and solid control volume (e.g., cathode gas and electrode-electrolyte assembly; anode gas and electrode-electrolyte assembly; anode gas and separator plate; separator plate and reformer stream). Note that radiation heat transfer between the electrode-electrolyte assembly and the separator plate is neglected because in the planar, co-flow, intermediate temperature fuel cell design, heat exchange is dominated by convection.

Temperatures and species mole fractions in the anode and cathode gas streams are determined from equations (1) and (2). Equation (3) is used to determine temperatures in the anode electrode plate, and electrolyte. To avoid algebraic equilibrium constraints, steam reformation chemical kinetics, based on the exit flow conditions are used in the reformer stream and anode control volume as was done in [16–18]. Electrochemical reaction rates in the SOFC are determined from the current, an input to the fuel cell model, based on Faraday's law and SOFC half reactions [16–18]. Details of the solution strategy for the fuel cell component can be found in [16–18].

From the fuel cell temperatures, and species mole fractions, quasi-steady electrochemistry is assumed to determine the SOFC voltage, based upon exit conditions of the fuel cell. The electrochemical voltage model presented in [16–18], is used; it accounts for Gibbs free energy, activation polarization, Ohmic polarization, and concentration polarization. The only difference from [16–18] is that a more detailed Ohmic polarization model adapted from [19] was used in the present model. This adaptation accounts for the temperature dependence of the overall fuel cell resistance as follows:

$$E_{ohm} = \frac{i}{A} \cdot T \cdot \exp\left(\frac{8700}{T} - 25.855\right) \quad (4)$$

Note that current is an input to the fuel cell and a single cell voltage is found thus avoiding algebraic voltage constraints.

## GAS TURBINE

The gas turbine is modeled as presented in [16], based on compressor and turbine performance maps to model the full operating range of the gas turbine. Maps for both efficiency and mass flow (as a function of normalized pressure ratio and rotational speed) are used for the compressor and turbine. The dynamics of the turbo-machinery are determined by the solution of two

equations that determine two dynamic states, (1) a dynamic torque balance on the gas turbine shaft,

$$\frac{d\omega}{dt} = \frac{P_{turbine} + P_{compressor} - P_{mtg}}{J\omega} \quad (5)$$

and (2) a dynamic molar conservation equation in the turbine.

$$\frac{d\left(\frac{PV}{RT}\right)}{dt} = \dot{N}_{in} - \dot{N}_{out} \quad (6)$$

Equation (6) is solved for the turbine inlet pressure. Equations (1)–(3), (5) and (6) represent the dynamic states of the system.

## STEADY STATE SYSTEM ANALYSIS

It is desired that the system operate safely and efficiently over a wide range of power conditions. To verify the systems' operating range, a steady state thermodynamic analysis was conducted. The ability to maintain the stack temperature, cathode inlet temperature, turbine inlet temperature, and turbine shaft speed within reasonable limits for the whole range of system operation was evaluated using the dynamic model described above. In all cases, the process was simulated until steady state was achieved.

For this study, the fuel is assumed to be pure methane and the ambient temperature is assumed constant at 298 K. The fuel cell was held at a constant fuel utilization of 85%. The stack temperature was maintained at 1000 K by varying the gas turbine shaft speed. In addition, the combustor outlet temperature was maintained at 1140 K by providing fuel to the combustor. Steady state simulation of the system showed that care must be taken to ensure operation of the gas turbine within its operating envelope.

This is because the amount of air cooling needed to maintain the fuel cell temperature varies greatly with the fuel cell operating power. At high power, the fuel cell generates much heat and the GT maximum shaft speed (97,000 RPM) is matched with the system's maximum operating power (275 kW). At low power, the fuel cell generates significantly less heat, and the fuel cell air cooling requirement is minimal (tends to zero). To control the fuel cell temperature at low power the gas turbine would have to operate at speeds less than its minimum speed for sustenance. This limitation has also been reported by [10] for topping SOFC/GT hybrid systems.

It is assumed that the gas turbine's minimum operating speed is 65 kRPM. Therefore the GT speed is controlled by manipulating the gas turbine power at or above 65 kRPM. Therefore, the fuel cell temperature can only be controlled by manipulation of the shaft speed until the 65 kRPM limit is reached. Once the gas turbine minimum shaft speed is reached, the fuel cell temperature is allowed to float. Note, that a gas turbine minimum operating speed of 65 kRPM is a conservative value and operation at lower RPMs should be possible.

Once the gas turbine minimum speed is reached, maintaining the combustor temperature by burning

supplementary fuel is particularly important in maintaining the cathode inlet temperature, and preventing the fuel cell from excessive cooling. This control strategy was found to allow the system thermodynamically to operate over a wide range of output power conditions with sustained gas turbine operation as shown in Figure 2.

With the designed gas turbine shaft speed constraint, and use of supplementary combustor fuel, it was found that the system was capable of operating from full power (275 kW) to power levels where only the gas turbine is generating power. While real hybrid systems must be capable of this wide performance range to enable safe start-up and shut-down, we limited our current investigation to system powers in the range of 70 to 275 kilowatts to analyze the system under dynamic operating conditions that are consistently in a hybrid operating mode where both GT and SOFC generate power.

Steady state analyses of the designed system, shown in Figure 3, indicate that the system meets the selected system operating requirements. Most importantly, the cathode inlet air temperature remained within 175 K of the fuel cell stack operating temperature. Additional simulations have indicated this would not have been the case without supplementary combustor fuel. The steady state analyses further indicate that the stack and turbine inlet temperatures can be well maintained over the range of operating power selected. Hybrid system efficiencies greater than 60% LHV can be achieved. However, due to significant use of fuel combustion, especially at low power operating conditions, the system efficiency at lower power becomes significantly less as indicated in Figure 3.

### INPUT-OUTPUT PAIRING

From the steady state analyses it is known that the system can operate over the full range of power within the system operating requirements. With the system configuration thus defined and with a proper operating range, it is essential to design a control strategy for rapid transient control capabilities that is robust to disturbances. Due to the complexity and nonlinear behavior of the hybrid system [5, 6], full state feedback type controllers that require state observers were not utilized in the presented research. Instead, a decentralized multi-loop feedforward-feedback type control strategy is designed.

To keep the system simple, no additional actuators are added. To gain the full benefit of a decentralized multi-loop controller, inputs and outputs must be paired properly. Each loop must be stable over the range of operating conditions and control loop interactions must be minimized. A prerequisite for input-output (I/O) pairing is to identify each reasonable and practical system input (manipulated variables) and the desired controlled system outputs (controlled variables).

### INPUT-OUTPUT IDENTIFICATION

The system, as designed, contains four actuators (inputs) that can easily be implemented in a real hybrid system: (1) GT load power, (2) supplementary combustor fuel flow, (3) fuel cell current, and (4) anode fuel flow. To

determine potential controlled system outputs, it is important to identify variables that common sensors can easily measure, such as temperatures, voltages, rotational velocities, and flowrates. Note that common, cost effective, and reliable sensors with rapid time response to measure fuel composition do not exist. This is a major concern of this research project, because it is desired to operate the system with fuel of varying composition. To resolve this problem, changes in composition can be inferred from fuel cell voltage measurements because cell voltage depends strongly on fuel composition. However, the following factors need to be considered as well: During operation, the fuel cell voltage depends on species' partial pressures in the anode and cathode compartments (due to the Nernst term), the amount of current being drawn from the fuel cell (due to polarizations), as well the stack temperature (mainly due to Ohmic polarization) and pressure conditions. Therefore, it is important to account for fuel cell current and temperature conditions to properly infer the fuel composition from voltage measurements. The usefulness of these measurements will become apparent once each control loop is designed; prior to this, however, I/O pairings must be established.

The desired outputs must be determined before I/O pairing can proceed. Assuming that changes in fuel composition can be inferred from voltage measurements, fuel cell voltage is selected as a desired output. Since the objective of the system is to meet external power demands, another desired output is the hybrid system power. During system design, it was determined that the combustor temperature indirectly impacts the cathode inlet temperature. To ensure that the combustor temperature does not exceed its maximum temperature (1150 K, operating requirement #5) it is selected as a controlled output. In the steady state analysis we concluded that the fuel cell temperature can be controlled via the gas turbine shaft speed. Therefore, both the turbine shaft speed and fuel cell stack temperature are selected as desired controlled outputs. In summary, five system parameters are to be controlled: (1) GT shaft speed, (2) stack temperature, (3) combustor temperature, (4) system power, and (5) fuel cell voltage. Each of the five system outputs is easily measurable by currently available sensors.

### RGA ANALYSIS

A total of four inputs

$$u = \begin{pmatrix} u_1 \\ u_2 \\ u_3 \\ u_4 \end{pmatrix} = \begin{pmatrix} \text{GT power} \\ \text{combustor fuel flow} \\ \text{fuel cell current} \\ \text{anode fuel flow} \end{pmatrix} \quad (7)$$

and five outputs

$$y = \begin{pmatrix} y_1 \\ y_2 \\ y_3 \\ y_4 \\ y_5 \end{pmatrix} = \begin{pmatrix} \text{GT shaft speed} \\ \text{stack temperature} \\ \text{combustor temperature} \\ \text{system power} \\ \text{fuel cell voltage} \end{pmatrix} \quad (8)$$

need to be paired. Physical insight leads to pairing  $(u_1, y_{1/2})$  and  $(u_2, y_3)$  where the former employs the already discussed cascade control structure. For the remaining inputs  $[u_3, u_4]$  and outputs  $[y_4, y_5]$  no such obvious pairing exists; both combinations  $[(u_3, y_4), (u_4, y_5)]$  and  $[(u_3, y_5), (u_4, y_4)]$  are viable options.

When pairing inputs and outputs for decentralized multi-loop feedback control, it is desired to minimize loop interactions [20]. This is accomplished by computing the system's relative gain array (RGA). RGA analysis provides a measure of the interactions caused by decentralized control using various I/O pairing choices [21]. Essentially, the RGA is a normalization of the transfer function, defined as:

$$RGA(G(w)) = \Lambda(G(w)) \equiv G(w) \mathbf{x} (G(w)^{-1})^T \quad (9)$$

where  $\mathbf{x}$  denotes element-by-element multiplication. The RGA can be used to measure diagonal dominance, by the simple quantity:

$$RGA\text{-number} = \|\Lambda(G(w)) - I\|_{sum} \quad (10)$$

To avoid instabilities caused by interactions in the crossover region, pairings that have an RGA-number close to 0 at these frequencies are preferred [20]. To determine the preferred pairing of inputs  $[u_3, u_4]$  and outputs  $[y_4, y_5]$ , the system was linearized over the range of operating power. Linearization is required because the RGA is a tool defined only for linear systems (see Equation 9). Because the current hybrid system is a highly nonlinear system, the process must be linearized for a large number of specific operating regimes. These operating regimes are characterized by their fuel cell current, spanning 1–50 Amps. The system was linearized around 75 specific system operating conditions. The RGA number was determined over the entire operating range for each of the two I/O pairings (Figure 4 and Figure 5).

As mentioned above, it is desired to choose a pairing with an RGA-number that is closest to zero at the crossover frequencies. This is not straightforward due to the large variation of time scales (see Table 1) and consequently the large variation of crossover frequencies. From the RGA of both pairings, shown in Figure 4 and Figure 5, respectively, it can be seen that pairing fuel cell current with voltage results in a less coupled system pairing at lower frequencies, but a more coupled system at higher frequencies.

Stiller et al. [5] determined that hybrid fuel cell systems can be stabilized despite strong interactions because of the difference in associated time scales. To allow fast control loops (current) to adjust to slower loops (flowrate), it is desired to decouple the system at high frequencies. Therefore, pairing system power with fuel cell current and fuel cell voltage with anode fuel flowrate is

preferred because it leads an RGA-number close to zero at high frequencies.

## CONTROLLER DESIGN & SIMULATED RESPONSES

### SYSTEM POWER CONTROLLER

The objective of this research is to meet a reference power demand ( $r_p$ ) by the system power ( $y_p$ ). Pairing system power with fuel cell current ( $u_i$ ) instead of fuel flowrate is beneficial because the fuel cell current generation time scale is almost instantaneous, while the time scale of species transport is on the order of seconds. This has the potential for enhanced system response.

Due to the need to track a large system operating range, a feedforward lookup table of current based on reference power signal is utilized in the system power controller. Note, that the required feedforward current ( $f_i$ ) is estimated from the previously determined steady state system operation. For robust tracking and disturbance rejection, a proportional plus integral controller is used for the system power. In addition to the feedforward and feedback control, the system power controller is designed with a power reference governor. The reference system power demand is lowered when the fuel cell operating voltage ( $y_v$ ) becomes less than a set voltage minimum ( $r_{vmin}$ ). This control feature is included to ensure safe fuel cell operating voltages, especially during transient load conditions. Manipulating the fuel cell current to control the system power output, with restriction on the fuel cell voltage is consistent with prior work done for topping SOFC/GT hybrid systems [5]. The system power controller is shown in Figure 6, and controller parameters are presented in Table 2.

To demonstrate the power controller's response, an instantaneous power increase from 70 kW to 250 kW was simulated. Note that each dynamic simulation is meant to demonstrate a particular controller performance, but each simulation presented in the paper is for the fully controlled system (i.e., all control loops closed). The simulated system response is presented in Figure 7. During the simulation, the GT power remained almost constant, such that the fuel cell power had to increase to meet the system power demand. Following the simulated increase in system power demand, the GT power remains almost constant until the fuel cell temperature reaches its normal operating temperature. This is because the shaft speed setpoint is initially maintained at 65,000 RPM by the GT cascade controller until the fuel cell stack temperature increases from the lower stack temperature of low power conditions. After the fuel cell reaches a higher operating temperature and requires more cooling, the GT shaft speed is allowed to increase above 65,000 RPM. The turbine inlet temperature, which dictates the gas turbine performance and output, remains unchanged while the shaft speed is constant (at 65,000 RPM) and remains almost unchanged thereafter. The turbine inlet temperature does not change because the air flow is essentially constant at a given constant shaft speed and combustor temperature is maintained by the combustor temperature controller.

In the simulation the system power increased by 90 kW almost instantaneously. However the system power was limited, by the power reference governor, because the SOFC cell voltage became close to 0.6 V. This significant voltage decrease is due to an increase in fuel cell current (to meet system power demand) at the lower fuel cell stack operating temperature. The decreased stack temperature results in higher fuel cell internal resistance, such that the SOFC cannot immediately generate the current needed to meet the system power demand (even if the system had been at steady state). Following the instantaneous increase in power, the system power slowly increases, almost proportionally with the fuel cell stack temperature, at a constant fuel cell voltage. The increase in fuel cell stack temperature causes the fuel cell internal resistance to decrease, and consequently allowing for a larger fuel cell current with the power reference governor controlled minimum fuel cell voltage. Once the system power is reached, the fuel cell power stabilizes, and the fuel cell voltage increases.

### THERMAL MANAGEMENT CONTROLLER

The thermal management controller contains two control loops, a GT cascade controller (Figure 8) to control fuel cell stack temperature and GT shaft speed, as well as a combustor temperature controller (Figure 9). Thermal control of a bottoming MCFC/GT hybrid system has been previously investigated by [3]. In this research [3] a cascade GT controller and a combustor temperature controller were each investigated independently but never together in the same hybrid system. The GT cascade controller presented in [3] resulted in steady state oxidizer temperatures that were too high while the combustor temperature controller resulted in steady state cathode inlet temperatures that were too low.

The current control strategy, designed with the insight from [3], is a combination of a GT cascade controller for shaft speed and fuel cell temperature, and an oxidizer temperature controller. Steady state analyses of the control strategy have already shown that the system can be maintained in a safe operating regime, avoiding the problems of too high an oxidizer temperature and too low a cathode inlet temperature discussed in [3]. The combustor temperature controller is straightforward. The supplementary combustor fuel flow ( $u_{Ncomb}$ ) is manipulated from a feedforward look up table based on system power demand, and a proportional feedback on measured combustor temperature ( $y_{Tcomb}$ ).

The GT cascade controller manipulates the GT shaft speed setpoint to maintain a constant fuel cell stack temperature. The desired GT shaft speed setpoint is achieved by varying the GT power. As mentioned above, a minimum shaft speed of 65 kRPM is maintained at all times. Both shaft speed setpoint and GT power are found by means of proportional feedback and a feedforward on the system power demand. To avoid integral error build-up during saturation and transients, integral feedback is not used. This result in a slight tracking error, but exact control of the stack and combustor temperatures is not

required. It was found that the tracking error was acceptable, in the sense that the system remained within operating requirements.

To demonstrate robustness of the thermal controller, a 30 °C diurnal ambient temperature variation from 5°C to 35°C was imposed as a boundary condition for the system operated at 250 kW system power. The simulation, presented in Figure 10, indicates that despite the variation in ambient temperature the fuel cell temperature is maintained well. This is accomplished by varying the gas turbine shaft speed with changes in ambient temperature. Although this results in a variation of generator power, the system power is tracked. Note that this type of robust performance over diurnal and/or seasonal ambient temperature variations is neither typical of hybrid systems nor easily achieved without the type of control strategies implemented herein.

### ANODE FUEL FLOW CONTROLLER

As stated in system operational requirement #3, sufficient fuel (hydrogen) must be maintained in the fuel cell anode compartment at all times. If anode hydrogen becomes depleted, the fuel cell voltage will drop precipitously and fuel cell power will be lost. More importantly, low fuel concentrations in the anode compartment can lead to irreversible anode oxidation that permanently damages the anode catalyst. It has been recognized that fuel cell hydrogen depletion during load transients can be minimized by current-based fuel control [17, 18]:

$$\dot{N}_{fc} = \frac{i \cdot n}{4 \cdot U_{set} \cdot 2 \cdot F \cdot 1000} \quad (11)$$

That is, one should control the anode fuel flow in proportion to the fuel cell operating current such that constant fuel utilization is maintained in the fuel cell. Essentially, this control technique is an anode fuel flowrate feedforward based on the current.

Controlling the fuel flow using a feedforward on current such as in Equation (11) will maintain constant fuel utilization as long as the fuel mixture is known [16, 17]. As can be seen from Equation (11) this is independent of system performance, as long as the ratio between fuel flow rate and current can be maintained. In the form Equation (11) is presented, the fuel is considered to be pure methane. However, since a fuel composition sensor is not available, if the fuel content ever changes with only a feedforward controller implemented, then the operating utilization will vary (possibly leading to hydrogen depletion in the anode compartment). As discussed earlier in the I/O section, fuel cell voltage can be utilized as an indicator of varying fuel composition.

The system's steady state power/fuel cell voltage relationship can be determined for a nominal fuel mixture and fuel cell operating conditions. In the present case, the nominal operating condition was taken to be pure methane fuel, at 298 K ambient temperature, and one atmosphere pressure (as in the steady state analysis). Note that the steady state power/fuel cell voltage



relationship does not account for variations in ambient temperature.

During operation, the voltage relationship can be utilized to indicate a below normal voltage at a given system power. If this is true then it is possible to control the anode fuel flow to maintain the operating voltage based on power. This can be accomplished by comparing the voltage feedback to the voltage determined from the system power relationship (Figure 11). Such a feedback ensures that if the fuel composition changes, sufficient fuel (hydrogen) will be present in the anode compartment.

As mentioned previously, the voltage can drop during operation not only because of fuel composition variations, but also because of below normal operating temperatures as well as higher than normal currents caused by transient conditions, varying ambient conditions and/or fuel cell degradation. However, voltage feedback is still beneficial because the system's thermal controller should be able to maintain the stack temperature at its normal steady state operating temperature. In addition, operating the fuel cell with slightly lower fuel utilization during transient conditions is beneficial to improve the response time, raising the voltage and allowing for higher current generation. In addition, operating the fuel cell at lower fuel utilization to compensate for fuel cell degradation, and ambient condition variation is not problematic except that it reduces overall system efficiency. During operation, the voltage can also be higher than normal. For example, after a power decrease, the anode compartment fuel concentrations may be temporarily higher than current flow and current conditions would otherwise suggest due to the volume of fuel that can be stored in the anode compartment. To avoid this kind of voltage feedback during dynamics associated with decreasing fuel cell power demand (and fuel flowrate), the voltage feedback can only increase the anode fuel flow rate.

Another issue of controlling the fuel flowrate from a voltage feedback is that during transient load conditions, as presented in Figure 7, the voltage can become saturated. Without precautions, this would result in an increase in fuel flow sent to the anode, and consequently increased fuel flow to the combustor. The combustor temperature would then increase too much, even if the combustor fuel were controlled to zero. To prevent such conditions, the anode fuel flowrate is lowered if the combustor temperature increases beyond 1050 K. To avoid integral wind-up, only a proportional feedback controller is used on the voltage. This is sufficient since tight control of the fuel cell voltage is not required.

To demonstrate the effectiveness of the voltage feedback, the fuel cell was operated at a constant 250 kW power output, on pure methane, at a constant 298 K ambient temperature. The fuel's methane content was then instantaneously decreased by 40%. The simulated system response is shown in Figure 12. A 40% instantaneous decrease in fuel methane content is very significant (greater than what would be typical in practice), yet the fuel cell hydrogen mole fraction remained almost constant through this transient, and the system power was

tracked almost perfectly. The fuel controller increased the anode fuel flowrate to compensate for the reduction in theoretical hydrogen content of the fuel. Although the change in fuel content was instantaneous, the anode fuel flow was increased over a period of about one minute since it takes some time for the anode compartment hydrogen concentration to drop in the fuel cell (due to mass storage) and consequently affect the fuel cell voltage (Figure 12). This suggests that practical mass flow controllers and plumbing equipment may provide fast enough a time response to control the system as designed herein.

The decrease in fuel utilization plotted in Figure 12 following the change in fuel content can be explained as follows. Utilization is defined in terms of flow rates and theoretical hydrogen content ( $\Theta$ ):

$$\Theta = 4X_{CH_4} + X_{CO} + X_{H_2} \quad (12)$$

$$U = 1 - \frac{\dot{N}_{out} \Theta_{out}}{\dot{N}_{in} \Theta_{in}} \quad (13)$$

Assuming equal inlet and outlet molar flow rates, a decrease in theoretical hydrogen content at the inlet will decrease the utilization. In this case, the amount of hydrogen will first decrease at the inlet causing a temporary decrease in utilization as defined (Figure 12). The amount of stored hydrogen within the fuel cell is essential for transient operation of fuel cells, because it provides a buffer for perturbation and delay in fuel actuation.

## DISCUSSION

One of the most useful features of a dynamic model that can incorporate the physics and chemistry associated with SOFC/GT systems is the ability to use the model to systematically evaluate the performance potential of a wide variety of system configurations. Initial analyses of the dynamic performance of several different system configurations were conducted in the initial phase of the current work. These analyses resulted in the selection of a hybrid cycle configuration that contained all of the required components, each with sufficient performance to enable the system to meet the above stated goals. The focus of this paper is the development and analysis of an effective control strategy after the system design had been completed.

To further demonstrate the system's transient load following capability and robustness, the control system's response to a varying power as well as varying ambient temperature, and fuel composition is analyzed (see Figure 13). The simulation results presented in Figure 14 indicate that the system is capable of load following with varying ambient and fuel concentration. During operation, the fuel utilization was maintained well in spite of the significant change in fuel composition or the load transients. With sufficient fuel, and the power reference governor enabled, the SOFC cell voltage is maintained above 0.6 V.

The simulation also indicates that the combustor temperature is kept at 1140 K during transient operation.

This results in the maintenance of a relatively constant stack temperature difference. During operation, the stack temperature always stays within operating constraints.

The designed control strategy has been shown to be robust with many design features that can be generally applied to other hybrid system designs. With the proposed controllers, the system has excellent transient load-following capabilities. Dynamic response could most likely be further improved by using more advanced model based controllers; this is part of ongoing research.

## SUMMARY & CONCLUSIONS

A system control strategy has been designed for a bottoming SOFC/GT hybrid system. The following results have been found:

- (1) The bottoming SOFC/GT hybrid system configuration is thermodynamically stable over a wide range of operating power conditions.
- (2) Proportional feedback of temperatures and voltage is sufficient to ensure safe operation of the system (i.e., integral action is not essential in temperature and voltage control loops).
- (3) Manipulating fuel cell current to meet system power is shown effective for system load following.
- (4) A gas turbine cascade control structure is shown to maintain robust control of the gas turbine shaft speed and fuel cell temperature during dynamic load variations and ambient temperature changes.
- (5) The addition and control of separate combustor fuel flow provides an effective means of minimizing fuel cell thermal gradients, and maintaining fuel cell temperature at low power.
- (6) Current based fuel control is an effective control strategy for avoiding fuel starvation in the fuel cell.
- (7) The hybrid system is shown to be robust to varying fuel composition by adjusting the fuel flow based on voltage feedback.
- (8) Relative gain array analysis proved useful for determining I/O pairings that minimize individual control loop interactions. The analyses indicate that for SOFC/GT hybrid plants that use voltage as a controlled variable, it is beneficial to control system power by fuel cell current and to control fuel cell voltage by manipulating the anode fuel flowrate.

## ACKNOWLEDGEMENTS

This research project is being performed under a Small Business Technology Transfer (STTR) project (No. DE-FG02-02ER86140) awarded by the US Department of Energy (DOE). The authors are pleased to acknowledge the guidance of Ms. Magda Rivera and Mr. Donald Collins of the National Energy Technology Laboratory (NETL), Morgantown, WV.

## REFERENCES

- [1] Mark C. Williams, Joseph. P. Strakey, Subhash C. Singhal, U.S. Distributed Generation Fuel Cell Program, *Journal of Power Sources* 131 (2004) 79-85.
- [2] Mark C. Williams, Joseph. P. Strakey, Subhash C. Singhal The U.S. Department of Energy, Office of Fossil Energy Stationary Fuel Cell Program, *Journal of Power Sources* 143 (2005) 191-196.
- [3] Rory A. Roberts, Jack Brouwer, Eric Liese, Randall S. Gemmen, Development of Controls For Dynamic Operation of Carbonate Fuel Cell-Gas Turbine Hybrid Systems, *Journal of Fuel Cell Science and Technology*, Accepted March, 2005.
- [4] Mario L. Ferrari, Loredana Magistri, Alberto Traverso, Aristide F. Massardo, Control System for Solid Oxide Fuel Cell Hybrid Systems, *Proceedings of GT2005*, ASME Turbo Expo 2005.
- [5] Christoph Stiller, Bjorn Thorud, Olav Bolland, Rambabu Kandepu, Lars Inslund, Control Strategy for a Solid Oxide Fuel Cell and Gas Turbine Hybrid System, *Journal of Power Sources* (2005).
- [6] G. Stephanopoulos, *Chemical Process Control- An Introduction to Theory and Practice*, Prentice-Hall Inc., New Jersey, 1984.
- [7] F. Marsano, L. Magistri, A. F. Massardo, Ejector Performance Influence on a Solid Oxide Fuel Cell Anodic Recirculation System, *Journal of Power Sources* 129 (2004) 216-228.
- [8] Mario L. Ferrari, Alberto Traverso, Loredana Magistri, Aristide F. Massardo, Influence of the Anodic Recirculation Transient Behavior on the SOFC Hybrid System Performance, *Journal of Power Sources* 149 (2005) 22-32.
- [9] P. Costamagna, L. Magistri, A. F. Massardo, Design and Part-Load Performance of a Hybrid System Based on a Solid Oxide Fuel Cell Reactor and a Micro Gas Turbine, *Journal of Power Sources* 96 (2001) 352-368.
- [10] J. Palsson, A. Selimovic, Design and Off-Design Prediction of a Combined SOFC and Gas Turbine System, *ASME Paper 2001-GT-0379*.
- [11] S. Kimijima, N. Kasagi, Performance Evaluation of Gas Turbine-Fuel Cell Hybrid Micro Generation System, *ASME Paper 2002-GT-30111*.
- [12] S.H. Chan, H.K. Ho, T. Tian, Modeling for Part-Load Operation of Solid Oxide Fuel Cell- Gas Turbine Hybrid Power Plant, *Journal of Power Sources* 114 (2003) 213-227.
- [13] I. Antepará, I. Villarreal, L.M. Rodríguez-Martínez, N. Lecanda, U. Castro, A. Laresgoiti, Evaluation of Ferritic Steels for Use as Interconnects and Porous Metal Supports in IT-SOFCs, *Journal of Power Sources* 151 (2005) 103-107.
- [14] Azra Selimovic, Miriam Kemm, Tord Torisson, Mohsen Assadi, Steady State and Transient Thermal Stress Analysis in Planar Solid Oxide Fuel Cells, *Journal of Power Sources* 145 (2005) 463-469.
- [15] Arata Nakajo, Christoph stiller, Gunnar Harkegard, Olav Bolland, Modeling of Thermal Stresses

and Probability of Survival of Tubular SOFC, Journal of Power Sources (2005).

[16] Roberts, R. A. and J. Brouwer, Dynamic Simulation of a Pressurized 220 kW Solid Oxide Fuel Cell-Gas Turbine Hybrid System: Modeled Performance Compared to Measured Results, Journal of Fuel Cell Science and Technology, Accepted August, 2005.

[17] Fabian Mueller, Jacob Brouwer, Faryar Jabbari, Scott Samuelsen, Dynamic Simulation of an Integrated Solid Oxide Fuel Cell System Including Current Based Fuel Flow Control, Journal of Fuel Cell Science and Technology, Accepted October, 2005.

[18] Fabian Mueller, Design and Simulation of a Tubular Solid Oxide Fuel Cell System Control Strategy, Masters Thesis, University of California Irvine, 2005.

[19] Jai-Who Kim, Anil V. Virkar, Kuan-Zong Fung, Karun Mehta, Subhash C. Singhal, Polarization Effects in Intermediate Temperature, Anode-Supported Solid Oxide Fuel Cells, Journal of The Electrochemical Society, 146 (1) 69-78 (1999).

[20] Sigurd Skogestad, Ian Postlethwaite, Multivariable Feedback Control, Analysis and Design, John Wiley and Sons, New York, 1996.

[21] Bristol, E. H., On a New Measure of Interaction for Multivariable Process Control, IEEE Transactions on Automatic Control, AC-11:133-134 (1966).

**FIGURES**

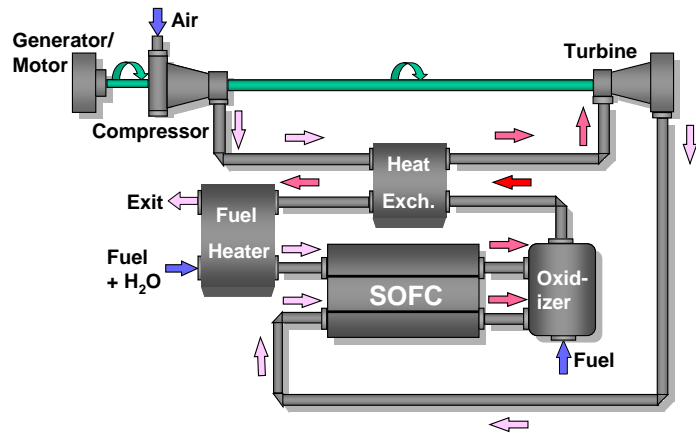


**Figure 1** Bottoming SOFC/GT hybrid system with variable speed GT and supplemental oxidizer fuel.

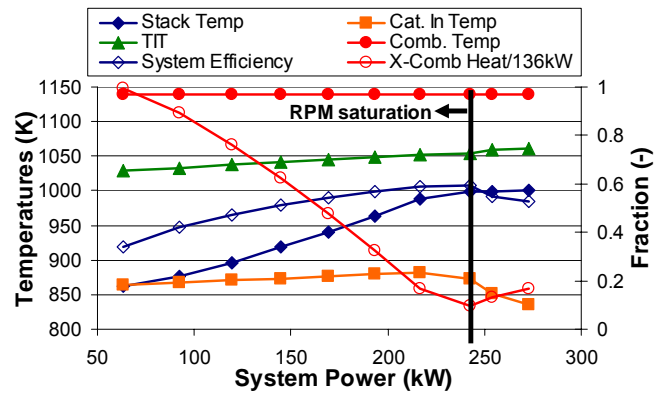


**Figure 3** Designed system steady state performances.

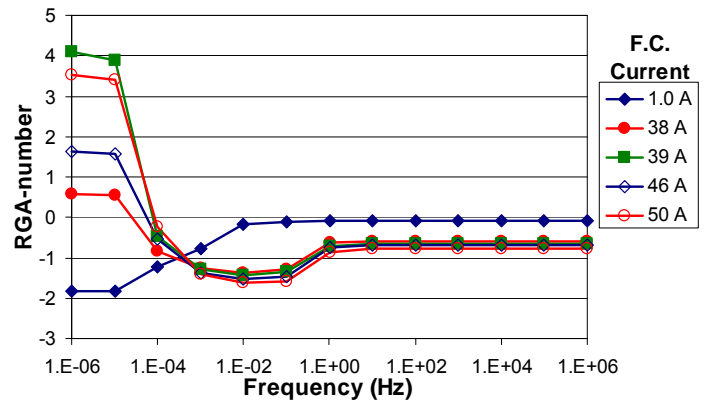


**Figure 4** Relative gain array analysis for fuel cell current-system power input and output pairing.

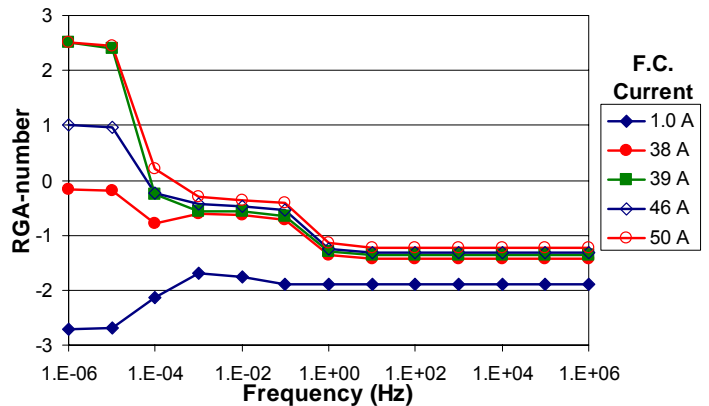


**Figure 5** Relative gain array analysis for fuel cell current-fuel cell voltage input and output pairing.

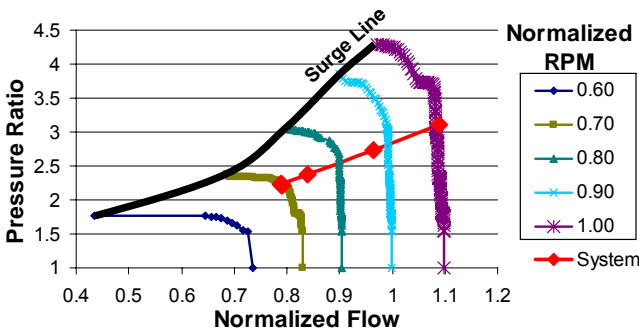


**Figure 2** Compressor flow map with operating points.

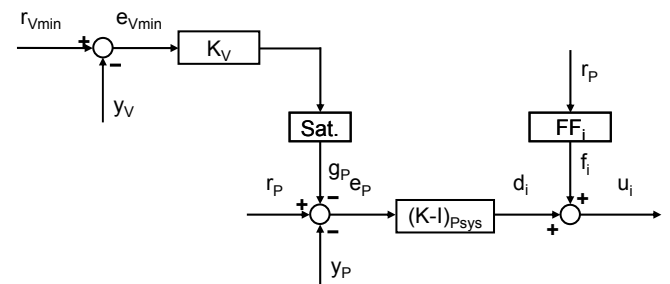


**Figure 6** System power controller.

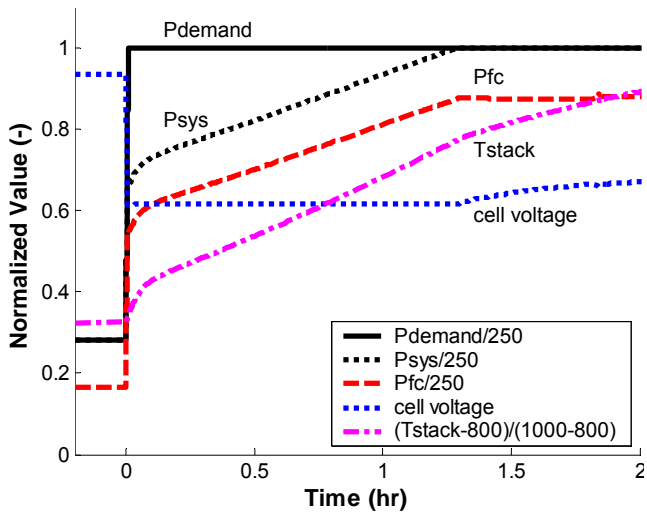


Figure 7 System response to an instantaneous power demand increase from 70 kW to 250 kW.

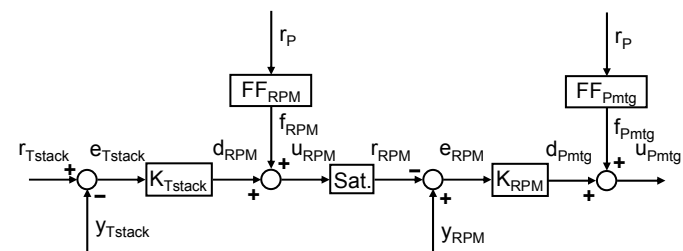


Figure 8 Gas turbine cascade controller.

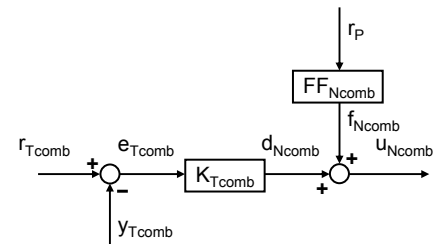


Figure 9 Combustor temperature controller.

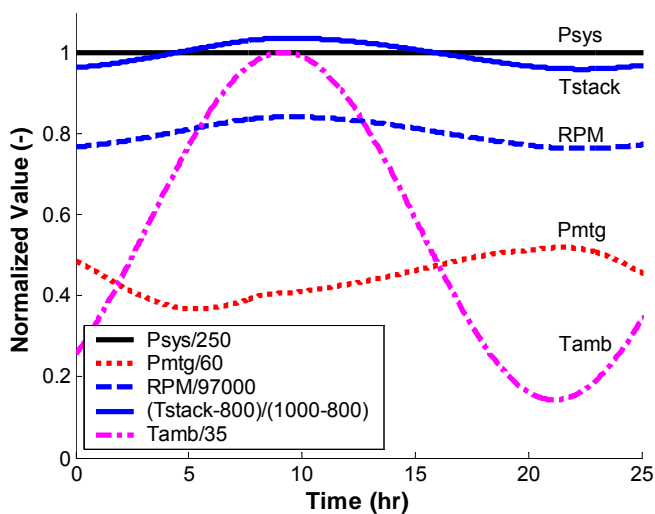


Figure 10 System response to ambient temperature variation from 5°C to 35°C.

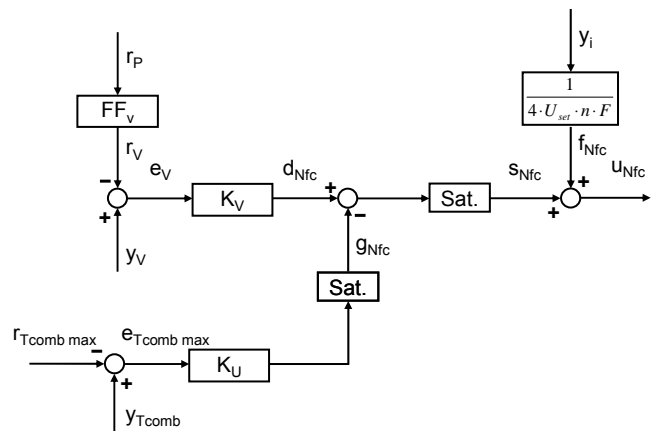


Figure 11 Anode fuel flow controller.

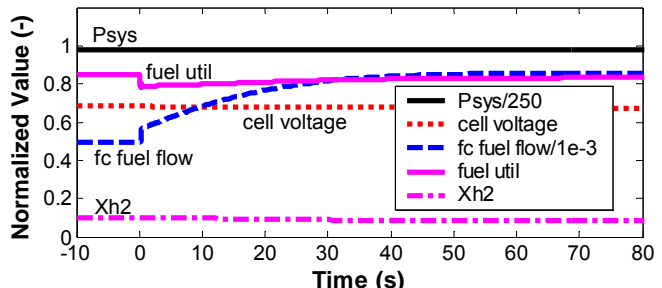
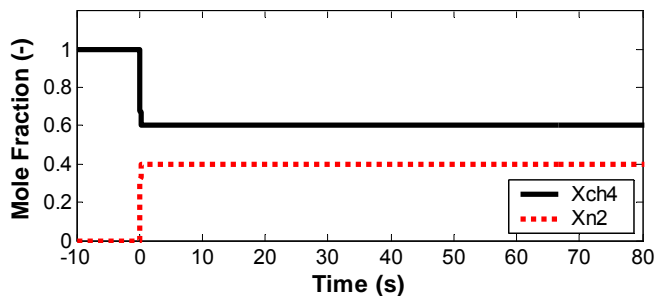


Figure 12 System response to an instantaneous 40% decrease in fuel methane mole fraction.

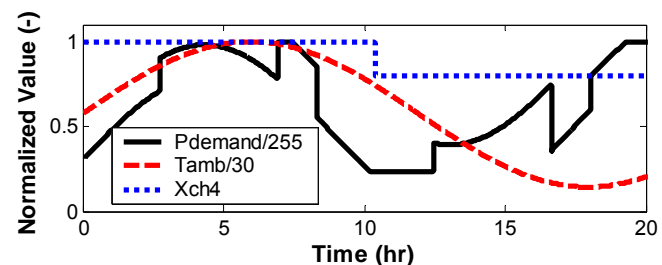
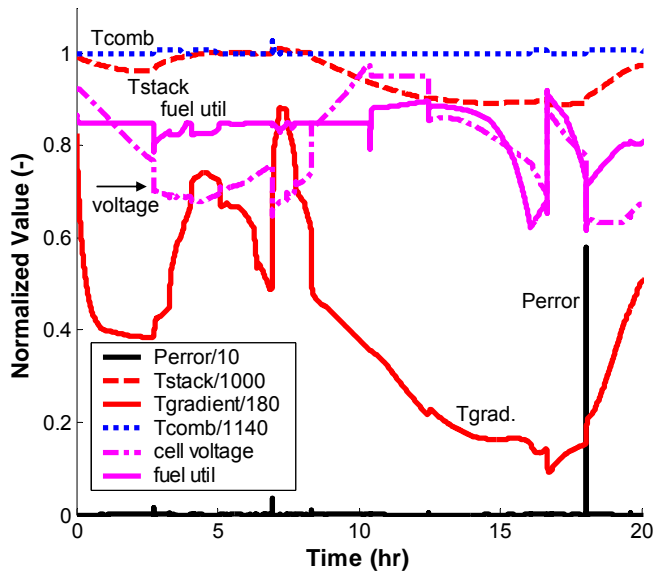


Figure 13 Simulated power demand, ambient temperature, and fuel methane mole fraction.



**Figure 14 Simulated system response conditions presented in Figure 13.**

**TABLES**

**Table 1 System relevant time scales, and there respective system model representation.**

RESPONSE	TIME SCALE	FREQUENCY	MODEL REPRESENTATION
Thermal	~hours	~0 hz	Equation (1) and (3)
Shaft inertia	~minutes	~0.01 hz	Equation (5)
Species conservation	~seconds	~1 hz	Equation (2) and (6)
Current generation	~instantaneous	~∞ hz	Quasi-steady assumption

**Table 2 Designed controller constants.**

**SYSTEM POWER CONTROLLER**

$r_{V_{min}}$	0.6 V	Fuel cell (cell) minimum voltage
$K_V$	5 kW/V	Fuel cell power reference governor gain
$K_{P_{sys}}$	10 A/kW	System power feedback proportional gain
$I_{P_{sys}}$	2 A/kW	System power feedback integral gain
Sat.	>0 kW	Power reference governor saturation

**GT CASCADE CONTROLLER**

$r_{T_{stack}}$	1000 K	Reference fuel cell operating temperature
$K_{T_{stack}}$	500 RPM/K	Temperature feedback proportional gain
Sat.	>65 kRPM	GT shaft speed saturation
$K_{RPM}$	0.1 kW/RPM	Shaft speed feedback proportional gain

**COMBUSTOR TEMPERATURE CONTROLLER**

$r_{T_{comb}}$	1140 K	Reference combustor operating temperature
$K_{T_{comb}}$	$1 \times 10^{-4}$ kmol/s/K	Combustor feedback proportional gain

**ANODE FUEL FLOW CONTROLLER**

$r_{T_{comb \ max}}$	1150 K	Reference combustor maximum temperature
$K_U$	0.2 kmol/s/K	Combustor temperature reduction gain
$K_V$	$5 \times 10^{-6}$ kmol/s/V	Fuel cell stack voltage feedback proportional gain
Sat.	>0 kmol/s	Anode fuel flowrate saturation
$U_{set}$	0.85	Fuel cell set operating fuel utilization